

Article

Reconstruction of Copper Smelting Technology Based on 18–20th-Century Slag Remains from the Old Copper Basin, Poland

Katarzyna Derkowska ^{1,*}, Mateusz Świerk ¹ and Kamil Nowak ²

¹ Institute of Geological Sciences, University of Wrocław, pl. Maxa Borna 9, 50-204 Wrocław, Poland; mateusz.swierk@uwr.edu.pl

² Institute of Archaeology, University of Wrocław, Szewska 48, 50-137 Wrocław, Poland; kamil.nowak@uwr.edu.pl

* Correspondence: katarzyna.derkowska@uwr.edu.pl

Abstract: This research was conducted on historical copper slags from Leszczyna and Kondratów in Lower Silesia, Poland. The area, formerly known as the Old Copper Basin, was a mining and smelting centre between the 18th and 20th centuries, with a dominant period in the 19th century. Cu-carbonates and residual chalcocite dominate local strata-bound copper deposits. Ore bodies are restricted to carbonate strata. A geochemical and mineralogical study of slag samples from four research sites allowed us to establish that a low amount of sulphur in slags results from S-poor ores, and pyrite with gypsum was implemented as reducing agents. Arkose sandstones served as a flux. During smelting, oxygen availability was limited, and temperature exceeded 1200 °C (18th- and 19th-century smelting) and 1400 °C (20th-century smelting). Calculated viscosity indexes mark the low efficiency of metal separation between the silicate and metallic phases. The skeletal and dendritic form of the crystals proved that slag melt was relatively rapidly cooled after formation, usually in air conditions. We estimated that approx. 2000 m³ of slag was created during the leading smelter (*Stilles Glück*) activity. The research provided various details of the historical copper smelting technological process in Leszczyna and Kondratów.

Keywords: non-ferrous archaeometallurgy; Cu-slag; geochemical tracers; reconstruction; Archaeometry



Citation: Derkowska, K.; Świerk, M.; Nowak, K. Reconstruction of Copper Smelting Technology Based on 18–20th-Century Slag Remains from the Old Copper Basin, Poland. *Minerals* **2021**, *11*, 926. <https://doi.org/10.3390/min11090926>

Academic Editor: Laura Chiarantini

Received: 1 August 2021

Accepted: 23 August 2021

Published: 27 August 2021

Publisher's Note: MDPI stays neutral with regard to jurisdictional claims in published maps and institutional affiliations.



Copyright: © 2021 by the authors. Licensee MDPI, Basel, Switzerland. This article is an open access article distributed under the terms and conditions of the Creative Commons Attribution (CC BY) license (<https://creativecommons.org/licenses/by/4.0/>).

1. Introduction

Pyrometallurgical slags are common metal smelting remains that record details of their origin in the matter of geochemical and mineralogical imprints pointing to the technological process of their production [1,2] or isotopic composition suggesting the metal deposit from which the ore was mined to be used in a given process [3,4]. Because historical metal smelting technological processes are rarely described in written sources, it is essential to reconstruct this technology based on accessible remains for the recognition of changing technology.

In historical times, the Old Copper Basin was one of the most important centres related to copper mining and metallurgy in Central Europe [5]. The first signs of mining activity in Kondratów and Leszczyna date back to the turn of the 15th and 16th centuries [6], but it is assumed that it started as soon as the 13th century [7]. The most significant development occurred in the 19th century when copper smelting was also carried out on site, namely the *Stilles Glück* smelter operating between 1865 and 1882 [8]. Numerous slag remains have been left in the surrounding environment due to historical smelting activity and are now a source of knowledge of the historical smelting process.

The first reconstruction studies focused on the Mediterranean region [9–12]. Several studies were already completed on metal smelting in Central Europe and Poland. These include the recognition of various metal smelting technologies, including Cu [13] Pb-Ag [1,14], Ag [10], and Zn [15]. After a three-year hiatus, reconstructions of the smelting

conditions have recently become acknowledged again [2,16,17]. Still, only a few papers on the reconstruction of historical base metal smelting from Poland have been published in the past, and there are no data regarding the important copper mining and smelting centre, which is the Old Copper Basin.

This article aims to reconstruct details of the metal smelting process in the Old Copper Basin in Poland in the 18–20th centuries. It also serves as an addendum to a recently published study by the same author [16], where the main focus was set on the temperature with a disregard for other elements of the metal smelting process. Reconstruction of all elements of the technological process is critical for proper recognition of changing technology in various parts of the world and future archaeological conclusions. The final aim of this article is to broaden our knowledge about the technological aspects of copper smelting between the 18th and 20th centuries in Central Europe.

2. Site Description

2.1. Geological Setting

The research area is located in Leszczyna Basin, placed in the SE edge of the North Sudetic Basin, a unit in the Kaczawskie Foothills area, north of the Sudetes Mountains and Bohemian Massif. The North Sudetic Basin is a sedimentary unit related to the Zechstein formation (mainly Zechstein Limestone Ca1) deposited in the Lower Permian due to Zechstein Sea transgressions to this area [18]. The unit is dominated by marls, limestones, and shales [7].

Copper ores mined in Poland belong to the strata-bound type (associated with sedimentary rocks) and appear near-surface in the SE edge of the North Sudetic Basin (the area of this study) and also approx. 1.4–2.2 km below ground level in the Fore-Sudetic Monocline, where current exploitation is carried out [19]. Because of a time difference in the mining activities, the North Sudetic Basin is also named the ‘Old Copper Basin’ (or ‘Old Copper District’), and deposits in the Fore-Sudetic Monocline are referred to as the ‘New Copper Basin’ (or ‘New Copper District’) [19].

Numerous researchers analysed the origin of the Kupferschiefer mineralization, and several theories were presented (e.g., [20–22]). It is currently accepted that Kupferschiefer mineralization results from the activity of two types of brines characterized by different chemical and physical parameters [23]. Mixing of these fluids led to a chemical reaction and gradual precipitation of metallic elements, mainly Cu, as a result of organic matter oxidation in the Kupferschiefer shales, and Pb in the adjacent zone where the highest pH occurred [23]. The Old Copper Basin deposits are dominated by copper carbonates with rare copper sulphides [24] and characterized by a lower grade (0.5–1 wt%), compared to the New Copper Basin, where within the bituminous shale of the Zechstein Kupferschiefer formation, Cu content reaches on average 1.5 wt% [25].

2.2. Historical Setting

According to some researchers, the extraction of copper ore in the Leszczyna Basin may have started as early as the 13th century [7,26]. However, the first historical documents confirming mining operations date back only to 1505 AD and concern a contract between the local authorities regarding the commencement of mining works in the vicinity of Kondratów (Site 2). Later records date to 1541 AD, when the area was leased for mining in the *Gottes Gabe* mine [27]. The mine in Kondratów was abandoned after 28 years of operation, and mining works were not resumed until the 18th century. At that time, the centre was developing intensively. Several mine shafts operated, and the extracted ore was smelted in the local smelting plant. Its operations are documented from the 1730s to the 1750s of the 18th century, although it probably lasted longer [7]. The development of mining and metallurgy in Leszczyna (Site 1) has been confirmed since 1661 AD when trial copper smelting was carried out and turned out unprofitable [26]. Mining activities resumed at the beginning of the 18th century when copper marl was mined. Later, one of the most important shafts called *Character* (*Charakterstollen*) was launched. Another was

the *Leszczyńska* (*Haseler*) adit (first half of the 18th century) [28]. It is possible that during the operation of the *Leszczyńska* adit, for the first time, regular copper smelting trials were carried out [7], but due to low profitability, the ore was later transported to another smelter. At the end of the 1860s, mining activities in Leszczyna intensified with the opening of a *Ciche Szczęście* (*Stilles Glück*) mine, and as a result, a smelter of the same name was built nearby with further attempts for local smelting [5,26]. The smelter operated together until the 1880s [26] and produced copper concentrate containing approx. 50% Cu, which was later transported for enrichment and pure metal smelting. In the history of mining in Leszczyna, there is one more period of return to the exploitation of copper ore, which took place in the 1950s with the construction of the Lena mine and associated smelter, which operated profitably until 1973.

3. Materials and Methods

3.1. Sampling

The material chosen for this study consists of slags and rocks (ores and ore-hosting rocks) collected in the vicinity of historical mining sites in Leszczyna and Kondratów. Approx. 30 kg of slag material was gathered from four distinguished sites to provide a representative amount of slag material. Twenty-six slag samples were selected for further analyses. The names of slag groups and waste piles are analogous to those distinguished by Kadziolka et al. [16], where variations in the chemical composition of local slags and suggested age variations between different waste piles are presented. Sites 1A and 1B are located near Leszczyna, in the northern part of the site, whereas Sites 2A and 2B are located near Kondratów village, in the southern part of the site (Figure 1).

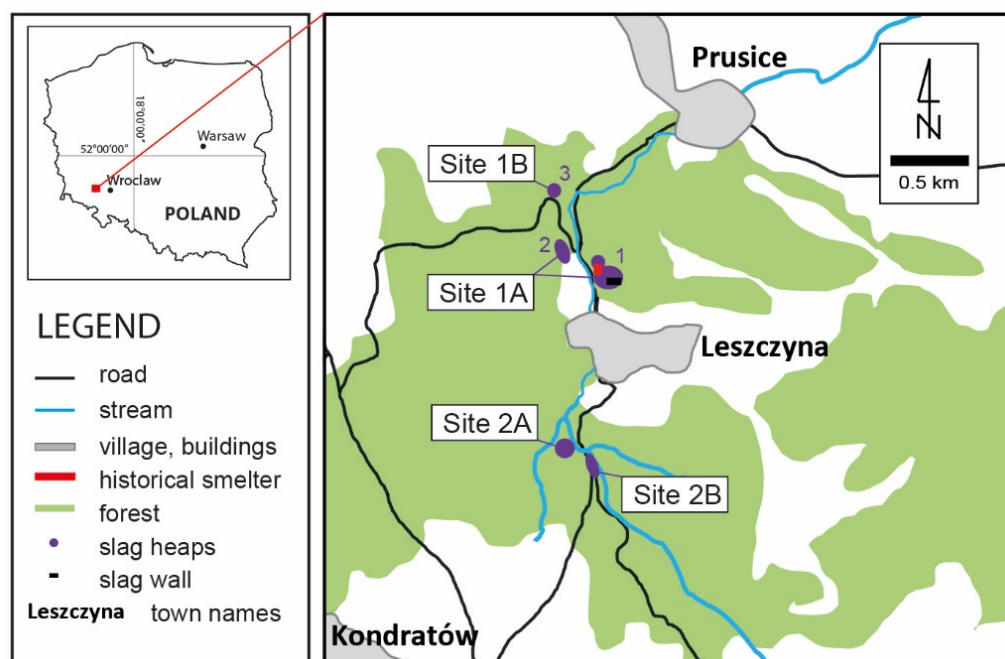


Figure 1. Research site location in Poland and the Leszczyna vicinity. Purple numbers (1, 2, 3) are mentioned in the text to distinguish different parts of the sites.

In Leszczyna, i.e., Sites 1A and 1B, three heaps were distinguished, two of which belong to the same production time (Heaps 1 and 2; Site 1A), and one (3; Site 1B) is younger. Heaps 1 and 3 are created of larger slag amounts than Heap 2 (Figure 1), where the material is present mainly on the surface (Figure 2C). The total heap area in Leszczyna reaches approximately 11,000 m². For the construction of the wall in the southern part of the site in Leszczyna (Figure 2A), approximately 6257 m³ of slag was used (the average dimensions of the blocks are 40 cm × 30 cm × 20 cm). Until today, the remains of long-term mining

activities, such as historical building support (Figure 2B) ground deformation or quarry remnants, are visible in the area [29].



Figure 2. Photographs presenting slags in Sites 1A and 1B surrounding. (A) Historical entrance to the mine shaft and slag wall (on the top-right part of the photo); (B) slags used as building support near the historical shafts; (C) big slag blocks at the 1B site.

The site in Kondratów is smaller and divided into two parts: Site 2A and Site 2B (Figure 1). Site 2A appears near the probable historical smelter and consists of slag material spread around the area's surface. The slag heap associated with Site 2B is present in the form of an embankment extending approx. 38 m along the stream. A 2020 study established that slags from the 2B site were created in Leszczyna, in the *Stilles Glück* smelter, as they highly resembled slags from Site 1A and were probably removed from the original place of storage. Thus, slags from Site 2B are dated to the 19th century, as they are Site 1A slags. The area of the slag ascent zone in Kondratów is approx. 210 m².

Rocks (ore-hosting rocks and ores) were collected from two sites: Leszczyna and Kondratów. In Leszczyna, rock outcrops are located west of Site 1A (Slags Heap 1) (Figure 1) and extend along the historical mining area presented in Figure 2A. In Kondratów, no rock outcrops are present. Instead, rock material is spread around the 2A site, similar to slag deposition. Altogether, five rock samples were collected, including four from Leszczyna and one from Kondratów.

Collected slag and rock material was cleaned with a rice brush under running water, air-dried for a week in a clean storage area, and divided with a diamond saw for thin section preparation and chemical analyses.

3.2. Chemical Analyses

All chemical analyses were executed in the Bureau Veritas Mineral Laboratories (BVM, ACME Lab, Vancouver, BC, Canada). Slag and rock samples selected for chemical analyses were crushed to $\geq 70\%$, passing 2 mm, and pulverized to $\geq 85\%$, passing 75 μm ,

according to laboratory regulations. Major and minor element content was determined with inductively coupled plasma–optical emission spectrometry (Spectro Ciros Vision ICP-OES) and inductively coupled plasma–mass spectrometry (PerkinElmer ELAN 9000 ICP-MS) after fusion with lithium borate ($\text{LiBO}_2/\text{Li}_2\text{B}_4\text{O}_7$) and dissolving with nitric acid (HNO_3). The detection limits for major elements are 0.01–0.04 wt% and are presented in detail in the laboratory catalogue at: http://acmelab.com/wp-content/uploads/2021/06/Bureau-Veritas-CAD-Fee-Schedule-2021-060221_compressed.pdf (accessed on 25 July 2021). LECO CS230 Induction furnace combustion analysis with the detection and upper limit between 0.02 and 50 wt% determined total S and C contents. Loss on ignition (LOI) was determined by weight difference after 4 h ignition at 1000 °C.

Reproducibility was calculated based on five replicate samples analyses by subtracting the value analysed in the sample from that in the replicate, dividing the result by the value analysed in the sample, and multiplying it by 100. The reproducibility values ranged from 0.23 to 2.19. Analytical accuracy was estimated with seven certified standard materials used in the BVM Laboratory: (1) Certified Reference Materials (CRMs): STD GS311-1 (Cu-Au ore, S and C reference material); STD GS910-4 (Ni sulphide ore, S and C reference material); STD OREAS134B (Zn-Pb-Ag reference material); STD GBM309-15 (Ore Grade Base Metal reference material) and (2) Internal Reference Materials: STD DS11 (reference material for Aqua Regia Digestion); STD OREAS45EA (reference material for Aqua Regia Digestion); STD SO-19 (reference material for Whole Rock Analysis). Reference materials were inspected to monitor the analytical accuracy with the calculations same as those used for assessing reproducibility and ranged from 0.07 to 3.70 for major elements.

3.3. Mineralogical and Petrographic Analyses

Slag and rock samples were subjected to mineralogical and petrographic analyses with 30 µm thick, uncovered thin sections. Materials were examined with Leica DM2500P and Zeiss Axiolab polarizing microscopes in transmitted light. The microscopic photographs were taken with a Canon G2 digital camera using Canon Remote Capture software. The modal composition was estimated using the JMicroVision program. The volumetric content of the glass, crystalline phases, metallic phases, pores, and secondary minerals were determined based on approx. 500 points for each sample on three representative and non-overlapping micrographs. For more detailed imaging and introductory chemical recognition, scanning electron microscope (SEM) examinations were performed using a JEOL JSM-IT100 SEM with an Oxford Instruments X-act energy-dispersive X-ray spectrometer (EDS) on carbon-coated thin sections. Experimental conditions were set at 15 and 20 kV accelerating voltage, 20 nA emission current, and 10–16 mm working distance with a high vacuum in the chamber.

Phase chemical analyses were conducted using a Cameca SX100 electron microprobe (EMPA) with a wavelength-dispersive spectrometer (WDS) detector and conditions set at 15 kV accelerating voltage, 10 nA beam current, and 10 s counting time. The following standards were implemented in the analyses: albite (Na), diopside (Mg, Si, Ca), orthoclase (Al, K), rhodonite (Mn), Fe_2O_3 (Fe), cuprite (Cu), sphalerite (Zn), rutile (Ti), YbPO_4 (P), crocoite-20 (Pb).

Identification of crystalline phases within glass-dominated samples was performed with a powder X-ray diffraction and the Xenocs WAXS/SAXS, EMPYREAN (PANalytical) X-ray powder diffractometer, which operated with CuK radiation at 40 kV with 40 mA in the range of 10° to 90° 2θ with a $1.2^\circ 2\theta \times \text{min}^{-1}$ counting time. PANalytical X'Pert HighScore software 2.0v with the PDF-2 ICDD (International Centre for Diffraction Data) database was used for pattern identification.

4. Results

4.1. Slag Overview

Macroscopically, samples from both sites are black and brown in colour and differ in porosity (Figure 3, Table 1). Leszczyna slags are most often found in medium (Site 1A) and

large (Site 1B) blocks, with a spherical and cubic shape (approx. 10–30 cm in diameter) and are distinguished by high porosity (pore diameter up to 1 cm); however, massive slags are also found at the 1A site. Kondratów slags (Sites 2A and 2B) are noticeably smaller, often irregularly shaped, and massive, with some highly porous samples (Figure 3).

In the microscopic image (Figure 4), the full range of structures can be distinguished: (1) the hyalite structure, dominated by glass (30% of the samples); (2) the dominant hypocrySTALLINE structure, consisting of glass and crystalline phases (63% of samples); and (3) almost holocrystalline samples (7% of samples). Among the hypocrySTALLINE slags, there are samples with high and low porosity (from 0.44 to 45.6 vol%). Hyalite slags are rather massive, and holocrystalline samples are porous (Table 1). The size of the crystalline phases varies from approx. 10 µm (based on BSE photographs) to 0.1–0.5 mm (Figure 5). Crystalline phases are most often formed as subhedral aggregates of small crystals, and the forms of single phase occurrence are highly differentiated, from dendritic, through skeletal and needle-like, to a few anhedral crystals (Figure 5). Metallic phases are also distinguished in the slags, and the set consists of metallic Cu, bornite, pyrrhotite, chalcocite, and chalcopyrite [30].

Table 1. Average modal composition of slags from four localities in the Old Copper Basin.

| | Site 1A | Site 1B | Site 2A | Site 2B |
|--------------------|--------------|--------------|--------------|--------------|
| | <i>n</i> = 5 | <i>n</i> = 2 | <i>n</i> = 6 | <i>n</i> = 2 |
| Glass | 47.92 | 89.47 | 52.37 | 84.72 |
| Crystalline phases | 36.29 | 8.80 | 31.17 | 9.31 |
| Pores | 13.69 | 1.40 | 16.03 | 5.85 |
| Metallic phases | 0.14 | 0.20 | 0.37 | 0.10 |
| Secondary phases | 0.38 | 0.10 | 0.12 | 0.05 |

4.2. Chemical Composition

Slag chemical composition is dominated by SiO₂ ranging from 42.5 to 49.8 wt% in samples from Leszczyna (Site 1A: 44.3 to 49.8 wt%; Site 1B: 42.5 to 43.2 wt%) and 43.8 to 49.0 wt% in samples from Kondratów (Site 2A: 43.8–48.3 wt%; Site 2B: 46.8–49.0 wt%) (Table 2). The main components also include: CaO (on average 19.1 wt%, 26.6 wt%, 17.2 wt%, and 20.1 wt% at Sites 1A, 1B, 2A, and 2B, respectively), Al₂O₃ (17.9 wt%, 16.2 wt%, 11.1 wt%, and 17.8 wt%), and Fe₂O₃, the content of which is significantly higher at Site 2A (3.5 wt%, 3.8 wt%, 15.6 wt%, and 2.7 wt% at Sites 1A, 1B, 2A, and 2B, respectively) (Table 2). The composition also includes noticeable amounts of K₂O (4.1–6.2 wt%) and MgO (2.0–3.1 wt%). The concentration of the remaining oxides does not exceed 1 wt%.

Copper content varies between the samples from different sites and is also diverse within one site (Table 2). The average concentrations at Sites 1A, 1B, 2A, and 2B reach 3573 mg/kg, 3688 mg/kg, 18,934 mg/kg, and 2207 mg/kg, respectively, with the highest amount discovered at the 2A site (18th-century smelting). Slag samples showed low sulphur content, which does not exceed 1 wt% in any of the analysed samples. On average, there is 0.42 wt% (Site 1A) and 0.25 wt% sulphur (Site 1B) in the slags from Leszczyna and 0.09 wt% (Site 2A) and 0.48 wt% (Site 2B) in slags from Kondratów (Table 2).



Figure 3. Macroscopic photographs of representative slags from four sites: Site 1A (19th-century smelting), Site 1B (20th-century smelting), Site 2A (18th-century smelting), and Site 2B (19th-century smelting). In the bottom row, two examples of ore-hosting rocks from Leszczyna are presented: Cu-marl and Cu-limestone.

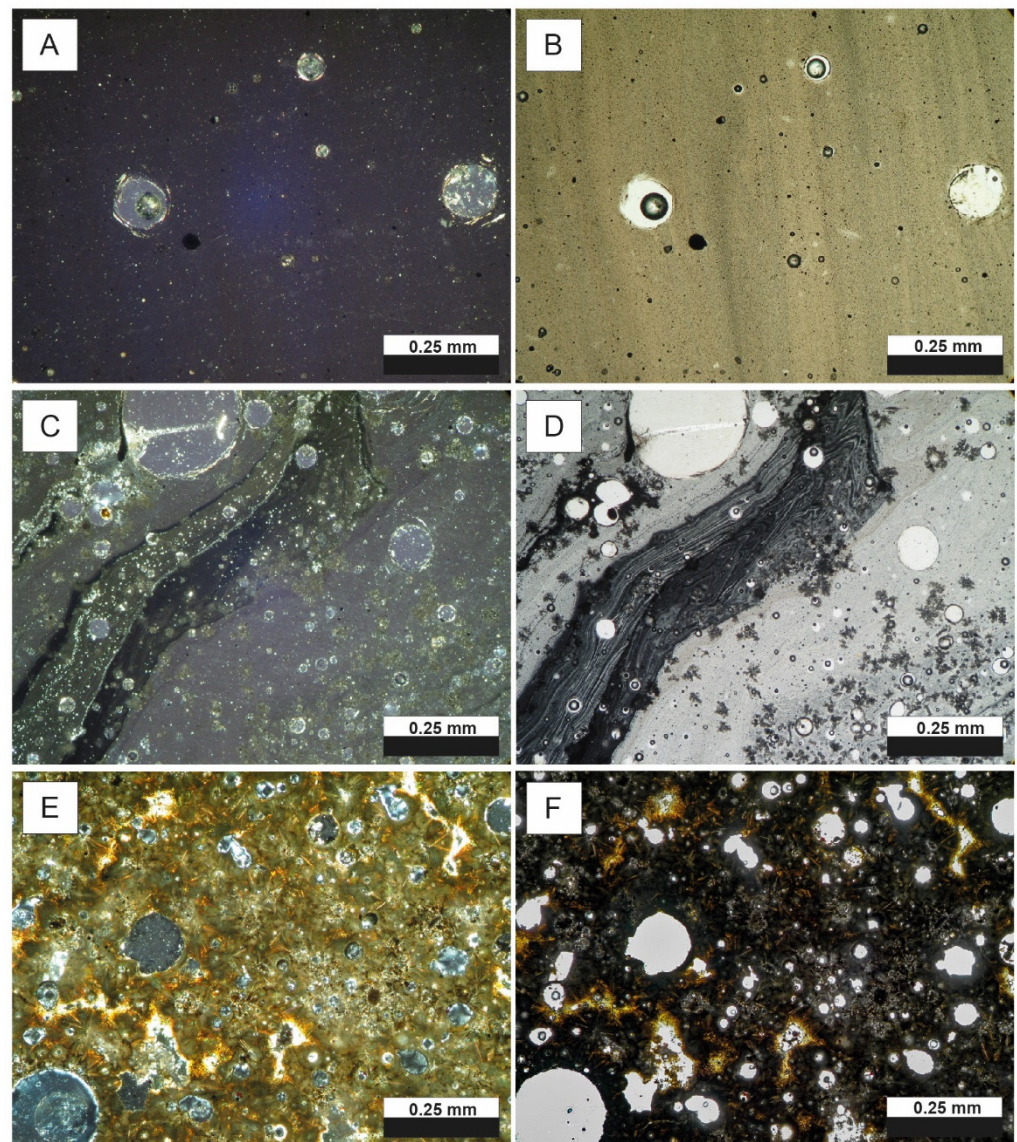


Figure 4. Microscopic images of slag samples in transmitted light in plane-polarized (left) and crossed-polarized light (right). (A,B) hyalite slags (glass and metallic phases (black)); (C,D) hypocrystalline slags (glass and crystalline phases); (E,F) holocrystalline slags (domination of crystalline phases).

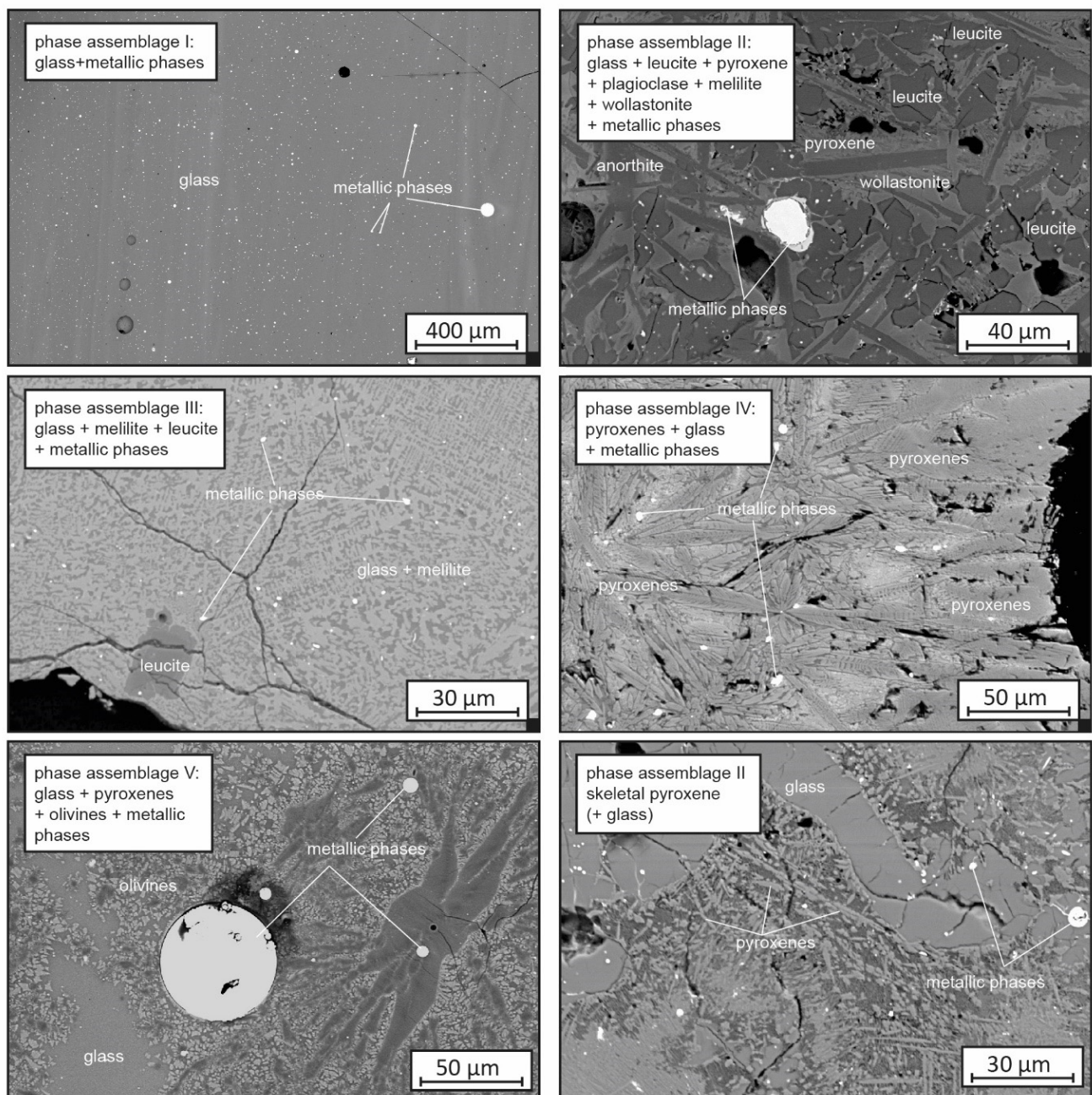


Figure 5. BSE images presenting different phase assemblages discovered in the analysed slags.

Table 2. Slags bulk chemical composition.

| | Site 1A (19th Century) | | | Site 1B (20th Century) | | | Site 2A (18th Century) | | | Site 2B (19th Century) | | |
|--------------------------------|------------------------|-------|--------|------------------------|-------|-------|------------------------|-------|--------|------------------------|-------|-------|
| | av. * | Min | Max | av. * | Min | Max | av. * | Min | Max | av. * | Min | Max |
| SiO ₂ | 47.25 | 44.28 | 49.79 | 42.69 | 42.45 | 43.24 | 46.03 | 43.84 | 48.33 | 48.08 | 46.84 | 49.02 |
| Al ₂ O ₃ | 17.94 | 16.77 | 18.89 | 16.20 | 16.03 | 16.41 | 11.06 | 9.57 | 12.99 | 17.78 | 17.30 | 18.16 |
| Fe ₂ O ₃ | 3.46 | 2.57 | 6.13 | 3.80 | 3.52 | 4.01 | 15.58 | 12.02 | 21.04 | 2.77 | 2.35 | 2.96 |
| MgO | 2.71 | 2.46 | 3.38 | 2.93 | 2.85 | 2.99 | 1.92 | 1.73 | 2.12 | 3.16 | 3.01 | 3.56 |
| CaO | 19.09 | 17.00 | 23.20 | 26.64 | 25.84 | 27.40 | 17.19 | 13.64 | 19.30 | 20.05 | 18.58 | 22.83 |
| Na ₂ O | 0.23 | 0.15 | 0.36 | 0.14 | 0.14 | 0.15 | 0.20 | 0.18 | 0.22 | 0.23 | 0.21 | 0.24 |
| K ₂ O | 6.27 | 5.85 | 6.70 | 5.59 | 5.40 | 5.71 | 4.06 | 3.41 | 4.86 | 6.22 | 5.77 | 6.50 |
| TiO ₂ | 0.79 | 0.74 | 0.83 | 0.72 | 0.71 | 0.74 | 0.55 | 0.50 | 0.61 | 0.82 | 0.79 | 0.84 |
| P ₂ O ₅ | 0.19 | 0.16 | 0.23 | 0.19 | 0.18 | 0.20 | 0.25 | 0.21 | 0.35 | 0.18 | 0.16 | 0.19 |
| MnO | 0.17 | 0.13 | 0.22 | 0.26 | 0.25 | 0.27 | 0.57 | 0.49 | 0.65 | 0.18 | 0.17 | 0.19 |
| Cr ₂ O ₃ | 0.01 | 0.01 | 0.02 | 0.01 | 0.01 | 0.01 | 0.01 | 0.01 | 0.01 | 0.01 | 0.01 | 0.01 |
| TOT/S | 0.42 | 0.21 | 0.93 | 0.25 | 0.21 | 0.32 | 0.09 | 0.05 | 0.19 | 0.48 | 0.30 | 0.63 |
| Cu | 3573 | 1503 | 10,760 | 3688 | 2627 | 5399 | 18,934 | 7330 | 44,159 | 2207 | 1856 | 2587 |
| v.i. * | 0.49 | 0.43 | 0.58 | 0.67 | 0.65 | 0.68 | 0.69 | 0.62 | 0.75 | 0.50 | 0.47 | 0.54 |

* av.—average; v.i.—viscosity index.

4.3. Phase Composition and Phase Chemistry

Five phase assemblages of slags with different phase compositions are distinguished (Figure 5).

The first assemblage includes samples from all sites (1A, 1B, 2A, and 2B) (35% of the analysed slags). In the phase composition, silicate glass and metallic phases are distinguished, sometimes with minor amounts of leucite. The glass chemical composition (Table 3) is dominated by SiO₂ (on average 41–49 wt%), CaO (approx. 18 wt%, except for one (HL2-1) sample, in which the average content exceeds 28 wt%), Al₂O₃ (approx. 11–18 wt%), and FeO, the content of which varies between the samples and reaches approx. 1012 wt% in slags from Site 2A (18th-century smelting) and 3 wt% in slags from Sites 1A, 1B, and 2B (19th- and 20th-century smelting). Similar to the bulk composition, high concentrations of K₂O (approx. 45 wt%) and MgO (23 wt%) are also distinguished in the glass. Numerous metallic phases appear in the first group in the form of round metal prills. The most common is metallic copper, and less often, chalcocite, bornite, and pyrrhotite are present.

The second phase assemblage consists of samples with a hypocrySTALLINE texture (Table 1) and a composition dominated by glass, leucite, Ca-rich pyroxenes, plagioclase, wollastonite, melilite, and esseneite (38% of the analysed slags). The glass of the second phase assemblage contains SiO₂ (on average 43.5 wt% in slags from Site 1A and 49 wt% from Sites 2A and 2B), CaO (average 24 wt% in all samples), Al₂O₃ (approx. 15.5 wt% in all samples), FeO (5 wt%), MgO (approx. 4 wt%), and occasionally a noticeable amount of K₂O (approx. 1.5 wt%) (Table 4). The most common phase in the second phase assemblage is leucite, present in the form of skeletal (cross) and rosette crystals approximately 100–500 µm in size (Figure 5). The chemical composition of leucite is dominated by SiO₂ (approx. 55 wt%), Al₂O₃ (approx. 23 wt%), and K₂O (approx. 20 wt%) (Table 4). Pyroxenes are common in these samples, although their share is smaller than that of leucite. Pyroxenes crystals are approx. 50–100 µm in size and are dominated by skeletal forms (Figure 5). The chemical variation of pyroxenes was presented elsewhere [16].

Table 3. Glass composition (Phase Assemblage I).

| Sample | Glass | | | |
|--------------------------------|--------|--------------------------|--------|---------------------------|
| | K2-3 | | HL2-1 | |
| | rep. * | average <i>n</i> = 43 | rep. * | average <i>n</i> = 141 |
| SiO ₂ | 48.55 | 49.15 | 41.10 | 41.30 |
| Al ₂ O ₃ | 18.27 | 18.59 | 15.60 | 15.40 |
| TiO ₂ | 0.89 | 0.86 | 0.70 | 0.70 |
| FeO | 3.22 | 1.87 | 3.10 | 3.10 |
| MnO | 0.16 | 0.19 | 0.20 | 0.30 |
| MgO | 2.95 | 2.94 | 2.60 | 2.70 |
| CaO | 17.93 | 18.59 | 29.00 | 28.60 |
| CuO | 0.09 | 0.07 | 0.00 | 0.10 |
| Na ₂ O | 0.25 | 0.23 | 0.10 | 0.10 |
| K ₂ O | 6.14 | 6.30 | 5.30 | 5.30 |
| P ₂ O ₅ | 0.15 | 0.16 | 0.20 | 0.20 |
| SUM | 98.58 | 98.95 | 98.20 | 98.00 |

* rep.—representative analysis.

Electron microprobe analyses identified additional phases occurring incidentally in slags of the second phase assemblage, including anorthite, wollastonite, melilites, and quartz. The chemical composition of anorthite is dominated by SiO₂ (approx. 47 wt%), CaO (approx. 29 wt%), and Al₂O₃ (approx. 17 wt%). Wollastonite consists of SiO₂ (approx. 50 wt%) and CaO (approx. 38 wt%), as well as a few percent of Al₂O₃, FeO, and MgO (Table 4). Numerous metallic phases are present in the samples with high variations in appearance, from round or oval to similar to a rectangle, or even completely irregular, in shape. The size of the phases ranges from approx. 50 μm to 0.5 mm. Within the second group, we recognized metallic copper, pyrrhotite, bornite, chalcocite, and cuprite, as well as metallic Fe, metallic Pb, and Fe-P, phases [30].

Table 4. EMPA results of phases analyses (Phase Assemblage II).

| Phase | Glass | | Leucite | | Pyroxene | | Anorthite | | Wollastonite | |
|--------------------------------|------------------------|-----------------------|------------------------|------------------------|------------------------|------------------------|------------------------|------------------------|------------------------|------------------------|
| | HL1 | HK6 | K2-4 | K2-11 | HK5 | PL6-s1 | K2-11 | HL2-3 | HK5 | |
| Sample | av. * <i>n</i> = 17 | av. * <i>n</i> = 4 | rep. * <i>n</i> = 4 |
| SiO ₂ | 43.50 | 49.00 | 54.42 | 55.54 | 48.55 | 40.74 | 47.30 | 44.80 | 44.82 | 49.49 |
| Al ₂ O ₃ | 15.56 | 15.80 | 23.22 | 23.66 | 12.59 | 8.85 | 31.45 | 34.11 | 32.75 | 0.72 |
| TiO ₂ | 1.48 | 0.70 | 0.05 | 0.08 | 2.32 | 1.02 | 0.11 | 0.07 | 0.21 | 0.19 |
| FeO | 5.75 | 4.35 | 0.00 | 0.11 | 3.12 | 19.74 | 0.28 | 0.17 | 0.76 | 5.56 |
| MnO | 0.28 | 0.94 | 0.04 | 0.06 | 0.17 | 0.63 | 0.00 | 0.13 | 0.01 | 0.89 |
| MgO | 5.36 | 3.13 | 0.00 | 0.03 | 7.58 | 3.91 | 0.51 | 0.38 | 0.35 | 1.61 |
| CaO | 25.40 | 23.10 | 0.07 | 0.27 | 20.16 | 23.25 | 17.69 | 18.72 | 18.53 | 41.03 |
| CuO | 0.07 | 0.19 | 0.15 | 0.05 | 0.00 | 0.09 | 0.04 | 0.04 | 0.00 | 0.18 |
| Na ₂ O | 0.16 | 0.26 | 0.13 | 0.09 | 0.13 | 0.12 | 0.90 | 0.30 | 0.25 | 0.05 |
| K ₂ O | 1.38 | 1.89 | 20.78 | 20.70 | 3.94 | 0.10 | 1.51 | 0.92 | 0.82 | 0.20 |
| P ₂ O ₅ | 0.24 | 0.33 | 0.00 | 0.00 | 0.11 | 0.45 | 0.05 | 0.00 | 0.07 | 0.12 |
| SUM | 99.18 | 99.69 | 98.86 | 100.60 | 98.64 | 98.95 | 99.82 | 99.64 | 98.57 | 100.03 |

* av.—average; rep.—representative.

The third phase assemblage is found only at the 1B site in Leszczyna (20th-century smelting). In the phase assemblage glass, melilites of various compositions, some leucite and metallic phases, are distinguished; however, most samples are dominated by glass (Table 1). The glass of the slags from the third group contains SiO₂ (approx. 43.5 wt%), CaO (27 wt%), Al₂O₃ (16 wt%), FeO (3 wt%), MgO (2.7 wt%), and K₂O (5.3 wt%). Melilites were characterized in detail elsewhere [16], but those found at the 1B site are Ca- and Al-rich,

granting a composition similar to alumoåkermanite $(Ca,Na)_2(Al,Mg,Fe)Si_2O_7$ (Table 5). Leucite composition does not vary from the results presented for prior phase assemblages. In the metallic assemblage, phases vary in composition and form, similar to those from the second group.

Table 5. EMPA results of phases analyses (Phase Assemblage III).

| Phase Sample | Glass | | Glass | | Melilite | | Melilite | |
|--------------------------------|--------|------------------------|--------|------------------------|----------|-----------------------|----------|-----------------------|
| | L2-6 | | L2-7 | | L2-6 | | L2-7 | |
| | rep. * | av. * <i>n</i> = 20 | rep. * | av. * <i>n</i> = 83 | rep. * | av. * <i>n</i> = 7 | rep. * | av. * <i>n</i> = 5 |
| SiO ₂ | 43.62 | 43.65 | 43.85 | 43.26 | 35.70 | 36.35 | 40.27 | 39.32 |
| Al ₂ O ₃ | 16.18 | 16.38 | 16.36 | 16.31 | 15.71 | 14.02 | 13.92 | 13.55 |
| TiO ₂ | 0.71 | 0.84 | 0.76 | 0.75 | 0.14 | 0.33 | 0.41 | 0.83 |
| FeO | 3.37 | 2.95 | 3.07 | 3.24 | 5.27 | 5.09 | 4.43 | 4.01 |
| MnO | 0.25 | 0.26 | 0.27 | 0.27 | 0.40 | 0.38 | 0.43 | 0.40 |
| MgO | 2.75 | 2.69 | 2.86 | 2.83 | 3.49 | 4.39 | 3.83 | 3.82 |
| CaO | 27.13 | 27.07 | 26.70 | 26.64 | 38.13 | 37.44 | 35.46 | 36.03 |
| CuO | 0.20 | 0.10 | 0.04 | 0.13 | 0.16 | 0.31 | 0.00 | 0.04 |
| Na ₂ O | 0.18 | 0.15 | 0.16 | 0.14 | 0.30 | 0.25 | 0.20 | 0.20 |
| K ₂ O | 5.34 | 5.36 | 5.43 | 5.24 | 0.57 | 1.03 | 0.89 | 0.78 |
| P ₂ O ₅ | 0.15 | 0.21 | 0.20 | 0.20 | 0.04 | 0.13 | 0.13 | 0.16 |
| SUM | 99.67 | 99.54 | 99.65 | 98.96 | 99.90 | 99.73 | 99.98 | 99.13 |

* av.—average; rep.—representative.

Two last phase assemblages were explicitly discovered at Site 2A. The fourth phase assemblage consists of samples dominated by glass and pyroxenes with marginal leucite participation (Figure 5). All of the recognized pyroxenes are Fe- and Ca-rich, generally similar to the diopside–hedenbergite composition. More details are given in the study by Kądziołka et al. [16]. The fifth group is represented by only one sample from the 2A site (in Kondratów) (HK2). The phase composition includes glass, abundant pyroxenes, fayalite, and tephroite. Fayalite and tephroite were discovered only with XRD analyses. The sample differs from other slags also in the microscopic image. It maintains the gradually passing contact of crystals embedded in the glass at the initial stage of crystallization (about 50 µm in size), with an almost completely crystalline part built from round, rosette-shaped, greenish-brown crystals up to 0.2 mm in size. The glass of this sample also differs visually from other groups, showing a stronger light-brown color. Microprobe studies highlighted the presence of two varieties of glass composition differing by approx. 10% of FeO and CaO compared to the previous phase assemblages. The glass is composed of SiO₂ (44.5 wt%), FeO (25.5 wt%), CaO (13 wt%), and Al₂O₃ (9.6 wt%). Two metallic phases were distinguished within the sample, bornite and chalcocite, which appear in a round form with a diameter of approx. 100 µm.

4.4. Ore-Hosting Rocks

Microscopic observations of rock samples showed slight textural differences in the presence of various allochemical components. Four types of rocks were distinguished: dolomitic limestone, dolomite, limestone, and marl/shale.

Gray dolomitic limestone (Sample SL1) presents a fine-grained, massive, and chaotic texture. Micrite carbonates dominate in the background. Additionally, there are small lithoclasts (dolomite and quartz crystals), reaching up to 0.1 mm, and a few skeletal fragments (sponge needles) up to 1.1 mm long. Opaque minerals commonly occur in an oval-like shape with irregular grain boundaries, reaching an average size of approx. 0.05 mm.

The dolomite is represented by Sample SL-2 (Table 6). It is a light-brown carbonate rock with a massive texture. The rock contains mainly fine-grained dolomite crystals (<0.05 mm), allochemes (round ooids with a size of approx. 0.2 mm), and elongated skeletal

fragments (sponge and shell needles) up to 1 mm. Irregular lumps up to 0.2 mm of opaque minerals are also found, as well as quartz and albite grains.

The PL2R2 sample represents limestone and is dominated by small calcite grains (<0.5 mm). The remaining samples, PL2R1 and SK1, are typical local Cu-marls. Samples are characterized by a directional texture defined by parallel lines filled with clay minerals that cross through the entire sample. The rock texture is heterogeneous, dominated by fine calcite crystals with an admixture of clay minerals (probably illite, as distinguished through XRD analysis). The composition also includes fine quartz (approx. 0.06 mm) and small opaque minerals, chalcocite and covellite (<0.05 mm).

Table 6. Rock chemical composition.

| | SL-1 | SL-2 | PL2-R1 | PL2-R2 | SK-1 |
|--------------------------------|-------|--------|--------|--------|--------|
| | L * | L * | L * | L * | K * |
| SiO ₂ | 7.41 | 2.97 | 25.46 | 9.98 | 24.86 |
| Al ₂ O ₃ | 2.25 | 0.57 | 9.04 | 3.48 | 8.89 |
| Fe ₂ O ₃ | 0.84 | 1.00 | 1.82 | 0.81 | 1.77 |
| MgO | 4.31 | 18.93 | 1.61 | 1.71 | 1.54 |
| CaO | 44.24 | 30.44 | 28.23 | 43.68 | 28.46 |
| Na ₂ O | 0.05 | 0.02 | 0.09 | 0.06 | 0.10 |
| K ₂ O | 0.88 | 0.13 | 3.43 | 1.35 | 3.66 |
| TiO ₂ | 0.10 | 0.02 | 0.41 | 0.14 | 0.38 |
| P ₂ O ₅ | 0.05 | 0.02 | 0.13 | 0.06 | 0.15 |
| MnO | 0.48 | 0.88 | 0.15 | 0.34 | 0.19 |
| Cr ₂ O ₃ | 0.00 | <0.002 | 0.01 | 0.00 | 0.01 |
| LOI | 38.50 | 28.20 | 45.00 | 26.10 | 37.30 |
| SUM | 99.12 | 98.20 | 99.94 | 96.55 | 98.90 |
| TOT/S | 0.29 | 0.01 | 0.41 | 0.06 | 0.04 |
| Cu | 5264 | 40 | 26,230 | 6060 | 10,400 |

* L—Leszczyna; K—Kondratów.

Rock chemical composition is dominated by CaO (30–44 wt% in Leszczyna and 28.5 wt% in Kondratów), SiO₂ (3–25 wt% in Leszczyna, 25 wt% in Kondratów), and MgO (4–19 wt% in Leszczyna, 1.5 wt% in Kondratów). There is also a noticeable amount of Al₂O₃ within the rocks (0.6–9.0 wt% in Leszczyna, 9.0 wt% in Kondratów) and Fe₂O₃ (0.8–1.8 wt% in Leszczyna, 1.8 wt% in Kondratów). Among the remaining oxides, a high concentration of K₂O is noted (3.4 and 3.7 wt%) (Table 6). The remaining oxides do not exceed 1 wt%. There is an apparent difference in the chemical composition of the rocks from the two localities. The differences in the concentration of the major element exceed 20 wt%, which suggests the considerable variability of the copper-bearing rocks over short distances (approx. 2 km). High loss on ignition (LOI) values were obtained for all samples, from 38.5% to 45% for the rocks from Leszczyna and 28.2% from Kondratów, which results from the high carbonates content in the rocks (Table 6).

Four out of five analysed samples presented high Cu concentration. The highest value was discovered in the Leszczyna marl presented in Figure 3 (ore-marl) and reached 26,200 mg/kg (Table 5). For the remaining rocks acquired at this site, concentrations of 6000, 5300, and 40 mg/kg are noted. The sample from Kondratów also contained a high Cu concentration exceeding 1 wt% (10,400 mg/kg).

5. Discussion

5.1. Historical Information

According to historical sources describing successive stages of ore preparation before the creation of the *Stilles Glück* smelter, the ore was crushed in pestles, floated, roasted, and melted with the addition of slag material and chalcopyrite from Miedzianka [26], another Cu mining and smelting centre located in SW Poland [13]. The production process resulted in copper matte creation, which was a purified Cu, Fe, and S alloy (with other components). Matte was used for subsequent roasting and smelting with enriched ore [7]. In the Leszczyna

surroundings (Prusice town, by the stream), historical constructions damming the water for crushing the excavated material were found [28]. The following chapters present conclusions about subsequent stages of metal smelting in the Leszczyna and Kondratów vicinity, based on slag analyses from the distinguished sites (1A, 1B, 2A, and 2B).

5.2. Furnace Input: Local Ores, Type of Flux, and Ore Roasting

Comparison of the chemical composition of copper-hosting rocks (ore) and slags allowed us to identify differences in the content of the major elements (Figure 6). For these comparisons and further conclusions, rock chemical compositions from two localities were averaged. This is because we discovered high variations in the ore chemistry (especially regarding the Cu content) (Table 6), and there were no explicit indicators of the ore composition at the time of its mining and smelting. Additionally, rocks presented in this study were collected from nearby locations, and such high chemical variations in one deposit are unlikely. More probably, the differences result from the fact that historical mining reached different parts of the deposit. We believe that the historical ore was more similar to two of the analysed samples, SK1 and PL2R1 (Table 6), as the first was collected from Kondratów (Site 2A, Figure 1), where mining was less advanced, i.e., not all high-grade ore was exploited, and Sample PL2R1 was acquired from the bottom of the soil profile based on the Cu-rocks in Leszczyna. Other samples could have been subjected to surface weathering.

Compared to rocks, slags from all sites (Figure 6) are CaO- and MgO-depleted and SiO₂-, Al₂O₃-, and Fe₂O₃-enriched. The high primary concentration of CaO and MgO in rocks is related to the composition of the dominant mineralogy calcite (CaCO₃) and dolomite (CaMg(CO₃)₂). The lime-rich composition restricted the necessity of using CaCO₃ as a melting agent, which was common in historical smelting [1,10,11]. The depletion of CaO and MgO in slags probably results from the addition of fluxes of different chemistry. Additionally, when the rock samples are considered individually, those with lower CaO and MgO content are Cu-enriched. Possibly, the historical ore was more enriched in sulphides, and its smelting resulted in decreased total carbonate content. In turn, the increase in SiO₂ and Al₂O₃ is a consequence of adding these components to the furnace as a flux, probably from various aluminosilicates. We assume that readily available rock material was used as the flux, namely local sandstones found in the immediate vicinity of Site 1A [26]. Arkose sandstones could also be a source of K₂O in slags, which is generally higher than in ores. The addition of sand was previously observed in numerous examples of historical metal smelting, e.g., in Poland [2], the Czech Republic [31], or South Africa [32]. In the case of the Old Copper Basin slags, the addition of sandstone flux would carry an unfavorable increase in melt viscosity (which is observed in slags and is discussed further). However, with low SiO₂ concentration in rocks (Table 6), its addition also facilitates slag creation through the creation of silicate melt in the furnace.

Historical documents indicate the use of gypsum (CaSO₄·2H₂O) and pyrite (FeS₂) as additional fluxes [7]. Although pyrite can be considered geochemically justified (a marked increase in the content of Fe₂O₃ in the slag, especially at Site 2A (Figure 6)), the addition of gypsum is less likely, at least for its Ca concentration. The high initial CaCO₃ concentration limited the need to use other additives containing calcium. However, gypsum and pyrite are desirable additions for their S content, which acts as a strong reducing agent during the metallurgical process required for carbonate- and sulphur-poor ores.

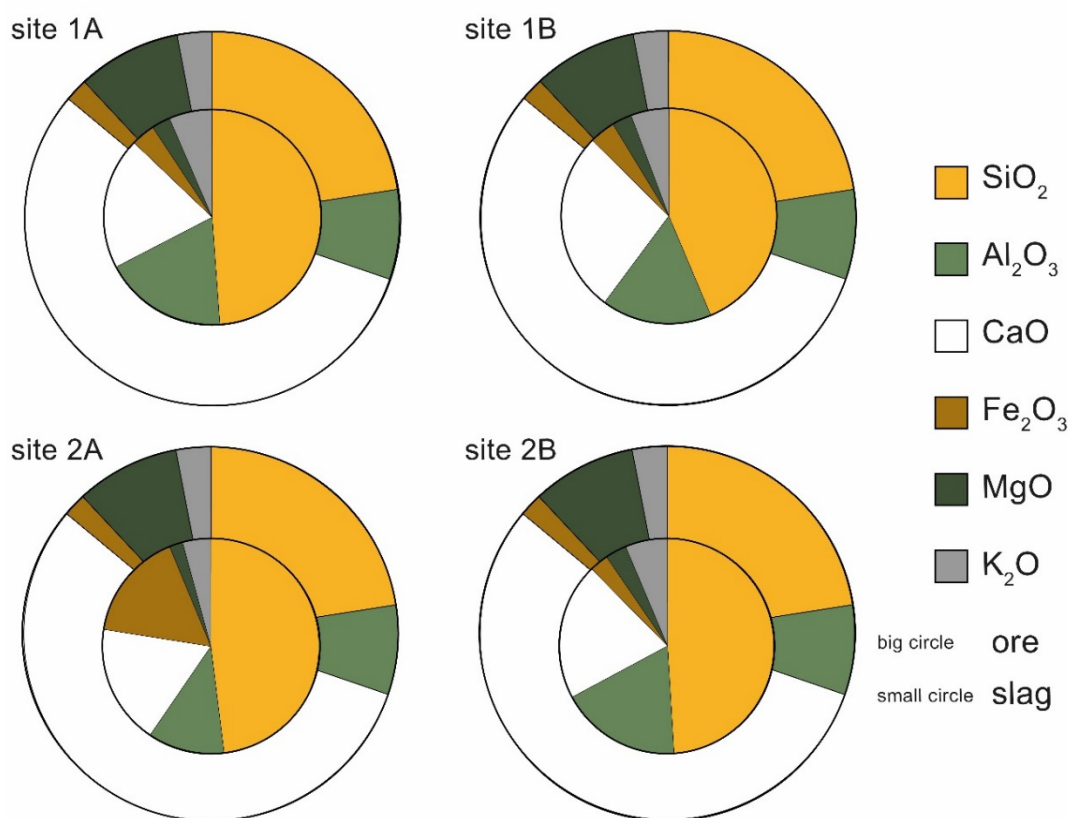


Figure 6. Comparison of ore (big circle in the background) and slag (small circle in the middle) percentage of major chemical components. Ore composition is calculated from all acquired rocks (as explained in the text), and slag composition is averaged for each site.

There are several theories regarding low sulphur content (<0.5 wt%) in slags, as values below 1 wt% are fairly common in historical smelting [1,4,31,33]. Most often, low S content proves that ore was pre-roasted before the further smelting activities. The presence of oxygen in the first stage of the process binds sulphur from sulphides, which is eventually removed from the furnace in gaseous form (SO₂) [10,33,34]. Additionally, ore roasting separates Fe from Cu (from iron-bearing copper sulphides) through the oxidation of Fe [35]. However, in the Old Copper Basin slags, low S content most probably results from the type of ore present in the area [4], as most Cu-bearing minerals are carbonates, not sulphides (Table 6). Additionally, except for the oldest 18th-century site 2A, where significant Fe-enrichment and S-depletion is observed, no straightforward imprints of ore roasting are found in the slags. We can only speculate that in the case of using more sulphide-enriched ore (e.g., if such variation appeared in the deposit), ore roasting would be necessary for metal sulphide oxidation. No signs of ore enrichment are noted in slags, which agrees with some of the historical documents [26].

5.3. Furnace Construction

According to historical sources [7], metal smelting in Leszczyna, especially the first smelting attempts, was conducted similarly to the Middle Ages, concerning the types of furnaces with only slight changes introduced in the furnace construction. In the description, however, we will focus on the furnaces of the *Ciche Szczęście* (*Stilles Glück*) smelter, which operated for a significant period of time and created most of the local slag remains.

At the beginning of operations in 1865, the smelter used a tall (approx. 5 m high) shaft Mansfield-style furnace, which was loaded from the top [7] (Figure 7). The material movement was influenced by gravity, and the furnace charge was transported down to the zones with increasingly higher temperatures. The most intensive combustion occurred

in the highest temperature zone, i.e., slightly lower than the blower nozzles, responsible for introducing additional oxygen. This area occurred at about a third of the shaft's height (from the bottom). As a result of the physicochemical changes in the furnace, metal and gangue minerals were separated in a liquid form. Every 6 h, the drain hole was pierced, and melt flowed down the gutter to one of the two settling tanks [7,8]. Due to the density differences, the lighter slag melt flowed to the top, and metal concentrate accumulated underneath.

By 1868, another three shaft furnaces were added to be further re-build in 1872, when taller round constructions with water cooling and a better heating system were introduced, which led to the more reducing atmosphere as well as higher temperatures achieved in the furnace [7,31].

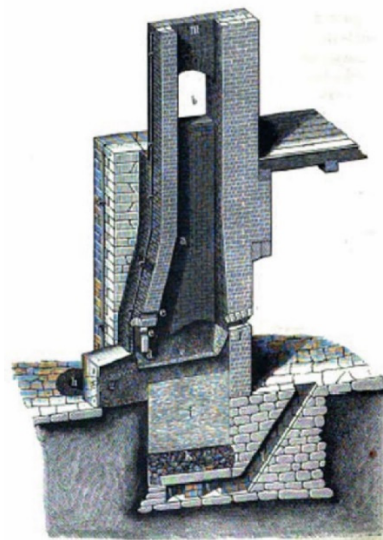


Figure 7. Simple shaft furnace. The construction is similar to the Mansfield-style furnaces that were used in Leszczyna. Drawing after Stolarczyk et al. [7].

5.4. Smelting Temperature

The problem of temperature reconstruction was analysed and described in detail in the 2020 article [16]. We suggested applying MELTS-Rhyolite software developed for thermodynamic reconstructions in the natural systems joined with the application of geothermometers and verification through the petrographic study. Until recently, most temperature reconstructions were based on the phase diagrams developed for major oxides (usually three or four) [4,36,37]. However, because slags present variable and complex chemical composition, it was often suggested that results are not exact enough to estimate the liquidus temperature of the specific slag (e.g., [4,12,13,36]). Thermodynamic modeling is more often introduced in reconstruction analyses [16,38,39], which allows assuming that future temperature reconstructions will become more exact. In a similar way, geothermometers based on the composition of various phases (e.g., pyroxenes [16]; pyroxenes, olivines and feldspars [40]; olivines-spinels [33]) help with the recognition of the cooling time for a given sample.

In the study, we discovered that slags from the three sites, 1A, 2A, and 2B, yielded similar liquidus temperatures. The 18th-century slags acquired from Site 2A recorded liquidus temperatures of approx. 1225 °C. The 19th-century slags from Sites 1A and 2B yielded slightly lower temperatures of about 1210 °C. The youngest 20th-century samples from Site 1B, on the other hand, recorded significantly higher liquidus temperatures reaching 1400 °C. For comparison, chemical diagram estimations yielded either similar temperatures for all analysed slags (diagram CaO–SiO₂–Al₂O₃: approx. 1300–1400 °C) or extremely high values for the 19th-century slags (diagram CaO–SiO₂–FeO: Sites 1A and 2B: 1436–1707 °C). For the 18th- and 20th-century samples, the diagram presented

temperatures of approx. 1440–1500 °C [16]. Our results agree with recent observations (both in the literature and experimental studies) that slags with higher lime content in the chemical composition tend to return higher liquidus temperatures [41].

5.5. Oxygen Fugacity (Furnace Atmosphere)

Depending on the historical period and technological advancement, the furnace atmosphere varied in historical smelting. Oxygen fugacity conditions can usually be recreated based on slag composition and presence of oxidized phases, namely iron silicates, due to the common presence of Fe phases in slags and its variation in the oxidation state [28]. Within our set of samples, several iron-rich mineral phases are observed: pyroxenes of the diopside–hedenbergite series ($\text{MgCa}(\text{Si}_2\text{O}_6)$, $\text{CaFe}(\text{Si}_2\text{O}_6)$), augite ($(\text{Al,Ca,Fe,Mg,Ti})_2(\text{Al,Si})_2\text{O}_6$), and (rarely) olivine: fayalite ($\text{Fe}_2(\text{SiO}_4)$). All of the mentioned minerals contain iron in the +2 oxidation state, which suggests limited oxygen availability during the final stage of smelting (reducing atmosphere). However, within some samples, esseneite (CaFeAlSiO_6) was also discovered (Table 7). This pyroxene contains 3+ iron in the composition, proving that some furnace leakage and oxygen availability appeared at Sites 1A and 2A (where the phase was identified). Still, most of the analysed samples were created in a reducing atmosphere with limited oxygen. We believe the observations to be reliable, as, in the presence of oxygen, iron oxidation takes place. In these situations, spinels, mainly magnetite, are often present [13]. Oxygen fluctuations could be pointed out by the presence of various iron oxides, e.g., magnetite, hematite, and wüstite [2].

The additional method is thermodynamic modeling, requiring introducing specific oxygen fugacity conditions for proper calculations. For the Old Copper Basin slags, the quartz–fayalite–magnetite (QMF) buffer was introduced and yielded reliable estimations in the phase composition [16].

Table 7. Representative esseneite analyses from Sites 1A and 2A.

| | Site 1A | Site 2A | Site 2A |
|--------------------------------|---------|---------|---------|
| | rep. * | rep. * | rep. * |
| Sample | HL1 | HK5 | K1-3 |
| SiO ₂ | 28.87 | 34.71 | 35.89 |
| Al ₂ O ₃ | 5.42 | 2.47 | 8.50 |
| TiO ₂ | 14.20 | 14.07 | 0.15 |
| Fe ₂ O ₃ | 26.40 | 26.88 | 30.27 |
| MnO | 0.50 | 0.49 | 1.25 |
| MgO | 8.36 | 2.99 | 0.00 |
| CaO | 15.90 | 14.02 | 17.89 |
| CuO | 0.05 | 0.42 | 0.04 |
| Na ₂ O | 0.05 | 0.28 | 0.65 |
| K ₂ O | 0.07 | 2.28 | 0.67 |
| P ₂ O ₅ | 0.17 | 0.51 | 1.03 |
| SUM | 99.99 | 99.11 | 96.33 |

* rep.—representative.

5.6. Slags Viscosity and Metal Extraction Efficiency

Viscosity is an important feature of slag material, as it provides information about the separation of silicate and sulphide (metallic) melt, which results in the effectiveness of the metal smelting process. Additionally, the range of slags viscosity gives an insight into differences between smelting episodes [42] or between different types of samples [13].

Several formulas for slags viscosity have been developed. For our study, the formula proposed by Bachmann [43] was used to calculate slag viscosity index. The value is calculated from the ratio of the viscosity-decreasing to viscosity-increasing oxides according to the equation:

$$\text{viscosity index (v.i.)} = (\text{CaO} + \text{FeO} + \text{MgO} + \text{MnO} + \text{K}_2\text{O} + \text{Na}_2\text{O}) / (\text{SiO}_2 + \text{Al}_2\text{O}_3)$$

The calculated results for the viscosity index are fairly similar at all sites and vary from av. 0.46 at Site 1B (20th-century smelting), through 0.50 and 0.52 (at Sites 2B and 1A, respectively (19th-century smelting)) to 0.68 at Site 2A (18th-century smelting). These results are exceptionally low compared to other historical slags (e.g., [1,9–11,29]), especially because they are derived from fairly young slag material. This means that the analysed set of slags is characterized by high viscosity (adverse to the v.i.). Values of this magnitude (approx. 0.50) indicate a low efficiency of metal separation between silicate and metallic phases. Low viscosity values in historical slags often result from a high concentration of oxides not included in the equation, e.g., PbO and ZnO, for which specific corrections were suggested [1,2,14]. However, because only insignificant amounts of other oxides are found within the analysed set of slags (Table 1), and oxides included in Bachmann's calculations constitute 96–98.5 wt%, we did not include the aforementioned corrections. Nonetheless, according to the calculated viscosity indexes, the separation of metal and silicate melt was on a low level, which is, however, not the case observed during a petrographic study. Metallic phases are most often present as separated, round metal droplets of various compositions (as described in Section 4), and only a negligible CuO concentration was analysed in the glass (Tables 3–5).

Large amounts of copper remained in the smelting wastes from the Old Copper Basin and provide additional information about the metal extraction efficiency. On average, slags contain approx. 2000–4000 mg/kg Cu at Sites 1A, 1B, and 2B (19th and 20th centuries) and almost 20,000 mg/kg Cu (2 wt%) at the oldest site 2A (18th century) (Table 2). These observations confirm the low level of metal recovery and worse extraction technology at the oldest site (2A) and point to the lack of significant improvements in 20th-century technology.

5.7. Cooling Conditions

After smelting, the slags were air-cooled. The microscopic observations of the structure allow for a preliminary estimate of the rate of crystallization, from sudden in the case of amorphous materials to slow, favoring the crystallization of mineral phases, especially at Sites 1A and 2A (Table 1). The analysed slags show large diversity, even within one site, which is most likely caused by collecting samples of the material from different cooling zones, including border zones, where contact with the environment was increased (thus the slag was cooling faster), and middle zones, where the phases were subjected to longer cooling. Samples from Sites 1B and 2B presented more amorphous slags, which proves the rapid cooling of the material. For the 20th-century 1B site, this most probably results from a more advanced cooling method. Slags discovered at Site 2B (19th-century smelting) could also represent materials created after introducing a new water cooling system [7]. A higher share of crystalline phases at Sites 2A (18th-century smelting) and 1A (19th-century smelting) probably results from not including any additional cooling system (Site 2A) and the creation of larger amounts of slag during a single smelting episode, which lowered the cooling rate for most of the slag melt.

5.8. Amount of Slag Created

The last element of the reconstruction of the smelting conditions was the reconstruction of the probable amount of slag produced in this area. Because not much of the historical data on the functioning of previous smelters survived, we only have detailed information for the 17 years of the operation of the *Stilles Gluck* smelter in Leszczyna, which created most of the local slag wastes. Based on the historical sources, about 1100 tons of copper concentrate were produced [7]. According to the previous study by Manasse and Mellini [10], the amount of metal obtained is 20% of the initial furnace charge. Assuming that the coke, which was the fuel, was added as 10–12% of the charge [7], and there were burnout components in the ore. The amount of slag obtained can be estimated at approximately 60% of the charge, i.e., approximately 3300–4000 tons of slag were produced. Taking into account the slag volume density, which is not high for such highly porous materials and

amounts to about 1.9 g/cm³ (1900 kg/m³), during the operation of the Stilles Gluck smelter, slightly over 2000 m³ of slag were produced and are spread in the area.

6. Conclusions

The conducted analyses made it possible to recreate in detail the conditions in which the metal smelting process was carried out in the Leszczyna and Kondratów copper smelters (Table 8). Significant diversity is noted in slag chemical and mineralogical composition. The variation results from the time differences in slag creation and the associated technology and ore chemistry characteristic. Strongly differentiated metal content in slags indicates differences in the technological level of the metallurgical process in two localities: metal recovery from ore was more effective in the younger Leszczyna centre (Sites 1A and 1B), as well as in Site 2B. The research made it possible to determine and confirm the approximate composition of the charge added to the furnace (carbonate ore, flux: probably local sandstone, pyrite, and gypsum as reducing agents). We confirmed the presence of oxygen during the final stages of smelting (furnace leakage), high temperatures reached in the furnaces (approx. 1200 °C and 1400 °C), as well as other details of the process, such as changing technology and cooling system for the creation of Site 1B slags. The research also made it possible to estimate the total volume of waste produced during the operation of the Leszczyna smelter (approx. 2100 m³).

Table 8. Summary of the metal smelting conditions at all distinguished sites.

| | Site 1A | Site 1B | Site 2A | Site 2B |
|-----------------------------------|--|--|--|--|
| Age | 19th Century | 20th Century | 19th Century | 18th Century |
| Location | Leszczyna | Leszczyna | Kondratów | Kondratów |
| Furnace input | Ore, coke, flux: arkose sandstones, pyrite, gypsum | Ore, coke, flux: arkose sandstones, pyrite(?), gypsum(?) | Ore, coke, flux: arkose sandstones, pyrite | Ore, coke, flux: arkose sandstones, pyrite, gypsum |
| Furnace type | Shaft furnace (Mansfield-style) | Unknown | Unknown | Shaft furnace (Mansfield-style) |
| Smelting (liquidus) temperature * | ~1210 °C | ~1400 °C | ~1225 °C | ~1210 °C |
| Oxygen fugacity | Reducing with leakage; QFM | Reducing; QFM | Reducing with leakage; QFM | Reducing; QFM |
| Viscosity index | 0.52 | 0.46 | 0.50 | 0.68 |
| Metal extraction efficiency | Low | Low | Low | Low |
| Cooling conditions | Air-cooled | Air-cooled (with water cooling system?) | Air-cooled | Air-cooled (possibly with water cooling system?) |

* Established in the Kądziołka et al. 2020.

Author Contributions: Conceptualization, K.D.; methodology, K.D.; validation, K.D., M.Ś., and K.N.; investigation, K.D., K.N., and M.Ś.; resources, K.D.; writing—original draft preparation, K.D.; writing—review and editing, K.D., M.Ś., and K.N.; visualization, K.D., and M.Ś.; supervision, K.D.; project administration, K.D.; funding acquisition, K.D. All authors have read and agreed to the published version of the manuscript.

Funding: This research was funded by the Polish Ministry of Science and Higher Education, Grant Number DI2015 023345 (Diamond Grant) to K.D. The APC was partially funded by the Institute of Geological Sciences, University of Wrocław.

Data Availability Statement: Data is contained within the article.

Acknowledgments: We would like to acknowledge that funding for this study was provided by the Polish Ministry of Science and Higher Education from budgetary funds for science in 2016–2018 as a

research project to K.D. under the Diamond Grant program (Decision: DI2015 023345). We would also like to thank J. Kierczak for the supervision of the initial part of this study. Additionally, we express our gratitude to two anonymous reviewers for their constructive comments, as well as to the editors Laura Chiarantini, Luke Wu, and Vivi Li.

Conflicts of Interest: The authors declare no conflict of interest.

References

- Ettler, V.; Červinka, R.; Johan, Z. Mineralogy of medieval slags from lead and silver smelting (Bohutín, Příbram district, Czech Republic): Towards estimation of historical smelting conditions. *Archaeometry* **2009**, *51*, 987–1007. [[CrossRef](#)]
- Warchulski, R.; Szczuka, M.; Kupczak, K. Reconstruction of 16th–17th Century Lead Smelting Processes on the Basis of Slag Properties: A Case Study from Sławków, Poland. *Minerals* **2020**, *10*, 1039. [[CrossRef](#)]
- Stos-Gale, Z.A.; Gale, N.H. Metal provenancing using isotopes and the Oxford archaeological lead isotope database (OXALID). *Archaeol. Anthropol. Sci.* **2009**, *1*, 195–213. [[CrossRef](#)]
- Chiarantini, L.; Benvenuti, M.; Costagliola, P.; Fedi, M.E.; Guideri, S.; Romualdi, A. Copper production at Baratti (Populonia, southern Tuscany) in the early Etruscan period (9th–8th centuries BC). *J. Archaeol. Sci.* **2009**, *36*, 1626–1636. [[CrossRef](#)]
- Kaczmarek, W.; Rożek, R. *Historia Poszukiwań i Rozpoznania Złóż rud Miedzi w “Starym Zagłębiu Miedziowym”*; Zagożdżon, P.P., Madziarz, M., Eds.; Dzieje Górnictwa—Element Europejskiego Dziedzictwa Kultury: Wrocław, Polska, 2008; pp. 97–104. (In Polish)
- Potysz, A.; Kierczak, J.; Pietranik, A.; Kądziołka, K. Mineralogical, geochemical, and leaching study of historical Cu-slugs issued from processing of the Zechstein formation (Old Copper Basin, southwestern Poland). *Appl. Geochem.* **2018**, *98*, 22–35. [[CrossRef](#)]
- Stolarczyk, T.; Kobylańska, M.; Kierczak, J.; Madziarz, M.; Garbacz-Klempka, A. *Leszczyna. Monografia Ośrodka Górnictwa i Metalurgii rud Miedzi*; Fundacja Archeologiczna Archeo: Radziechów, Polska, 2009. (In Polish)
- Festenberg-Packisch, H. *Der Metallische Bergbau Niederschlesiensunter Benutzungamtlichen Quellen in Geognostischerhistorischer und Technischer Beziehung*; Verlag von Moritz Perles: Vienna, Austria, 1881.
- Manasse, A.; Mellini, M.; Viti, C. The copper slags of the Capattoli Valley, Campiglia Marittima, Italy. *Eur. J. Mineral.* **2001**, *13*, 949–960. [[CrossRef](#)]
- Manasse, A.; Mellini, M. Archaeometallurgic slags from Kutná Hora. *Neues Jahrb. Miner. Abh.* **2002**, *8*, 369–384. [[CrossRef](#)]
- Manasse, A.; Mellini, M. Chemical and textural characterisation of medieval slags from the Massa Marittima smelting sites (Tuscany, Italy). *J. Cult. Herit.* **2002**, *3*, 187–198. [[CrossRef](#)]
- Bassiakos, Y.; Catapotis, M. Reconstruction of the Copper Smelting Process Based on the Analysis of Ore and Slag Samples. *Hesperia Suppl.* **2006**, *36*, 329–353.
- Kierczak, J.; Pietranik, A. Mineralogy and composition of historical Cu slags from the Rudawy Janowickie Mountains, Southwestern Poland. *Can. Miner.* **2011**, *49*, 1281–1296. [[CrossRef](#)]
- Ströbele, F.; Wenzel, T.; Kronz, A.; Hildebrandt, L.H.; Markl, G. Mineralogical and geochemical characterization of high-medieval lead–silver smelting slags from Wiesloch near Heidelberg (Germany)—An approach to process reconstruction. *Archaeol. Anthropol. Sci.* **2010**, *2*, 191–215. [[CrossRef](#)]
- Warchulski, R.; Gawęda, A.; Kądziołka-Gawel, M.; Szopa, K. Composition and element mobilization in pyrometallurgical slags from the Orzeł Biały smelting plant in the Bytom—Piekary Śląskie area, Poland. *Miner. Mag.* **2015**, *79*, 459–483. [[CrossRef](#)]
- Kądziołka, K.; Pietranik, A.; Kierczak, J.; Potysz, A.; Stolarczyk, T. Towards better reconstruction of smelting temperatures: Methodological review and the case of historical K-rich Cu-slugs from the Old Copper Basin, Poland. *J. Archaeol. Sci.* **2020**, *118*, 105142. [[CrossRef](#)]
- Chiarantini, L.; Benvenuti, M.; Bianchi, G.; Dallai, L.; Volpi, V.; Manca, R. Medieval Pb (Cu-Ag) Smelting in the Colline Metallifere District (Tuscany, Italy): Slag Heterogeneity as a Tracer of Ore Provenance and Technological Process. *Minerals* **2021**, *11*, 97. [[CrossRef](#)]
- Hara, U.; Słowakiewicz, M.; Raczyński, P. Bryozoans (trepostomes and fenestellids) in the Zechstein Lime stone (Wuchiapingian) of the North Sudetic Basin (SW Poland): Palaeoecological implications. *Geol. Q.* **2013**, *57*, 417–432. [[CrossRef](#)]
- Oszczepalski, S.; Speczik, S.; Zieliński, K.; Chmielewski, A. The Kupferschiefer Deposits and Prospects in SW Poland: Past, Present and Future. *Minerals* **2019**, *9*, 592. [[CrossRef](#)]
- Vaughan, D.J.; Sweeney, M.; Diedel, G.F.R.; Harańczyk, C. The Kupferschiefer: An overview with an appraisal of the different types of mineralization. *Econ. Geol.* **1989**, *84*, 1003–1027. [[CrossRef](#)]
- Wodzicki, A.; Piestrzyński, A. An ore genetic model for the Lubin-Sierszowice mining district, Poland. *Miner. Depos.* **1994**, *29*, 30–43. [[CrossRef](#)]
- Blundell, D.J.; Karnkowski, P.H.; Alderton, D.H.M.; Oszczepalski, S.; Kucha, H. Copper Mineralization of the Polish Kupferschiefer: A proposed basement fault-fracture system of fluid flow. *Econ. Geol.* **2003**, *98*, 1487–1495. [[CrossRef](#)]
- Kucha, H.; Pawlikowski, M. Badania genezy cechsztyńskich złóż miedzi w Polsce. *Geologia* **2010**, *36*, 513–538.
- Oszczepalski, S. Origin of the Kupferschiefer polymetallic mineralization in Poland. *Miner. Depos.* **1999**, *34*, 599–613. [[CrossRef](#)]
- Malon, A.; Tymiński, M.; Mikulski, S.Z.; Oszczepalski, S. Metal resources. In *The Balance of Mineral Resources in Poland as of 31.12.2018*; Szuflicki, M., Malon, A., Tymiński, M., Eds.; Państwowy Instytut Geologiczny: Warszawa, Poland, 2018; pp. 51–68. (In Polish)

26. Piątek, E.; Piątek, Z. *Tradycje Górnicze Ziemi Złotoryjskiej. Złotoryjskie Towarzystwo Tradycji Górniczych*; Wydawnictwo Atut: Wrocław, Poland, 2004.
27. Stolarczyk, T. *Górnictwo rud Metali Nieżelaznych na Dolnym Śląsku od XIII do Początku XVII w.* Ph.D. Thesis, Uniwersytet Wrocławski, Wrocław, Poland, 2009. (In Polish).
28. Stolarczyk, T. *Wyniki Badań Reliktów Dawnego Górnictwa Miedzi na Terenie Pogórza Kaczawskiego w Roku 2012*; Zagożdżon, P.P., Madziarz, M., Eds.; *Dzieje Górnictwa—Element Europejskiego Dziedzictwa Kultury*: Wrocław, Polska, 2013; Volume 5, pp. 339–351. (In Polish)
29. Kowalski, A.; Maciejak, K.; Wojewoda, J.; Kozłowski, A.; Raczyński, P. Anthropogenic changes of the “Old Copper Basin” area landscape (North-Sudetic Synclinorium) in the light of LiDAR-based geomorphometric analysis and archival data. *Biul. Państw. Inst. Geol.* **2017**, *469*, 177–200. [[CrossRef](#)]
30. Kaździółka, K.; Kierczak, J.; Pietranik, A. Charakterystyka mineralogiczna faz metalicznych z miedziowych żużli hutniczych Starego Zagłębia Miedziowego. [Mineralogical characteristics of metallic phases in copper slags from the Old Copper Basin, Poland]. *Prz. Geol.* **2019**, *67*, 164–166.
31. Ettler, V.; Johan, Z.; Zavrel, J.; Wallisová, M.S.; Mihaljevic, M.; Šebek, O. Slag remains from the Na Slupi site (Prague, Czech Republic): Evidence for early medieval non-ferrous metal smelting. *J. Archaeol. Sci.* **2015**, *53*, 72–83. [[CrossRef](#)]
32. Rozendaal, A.; Horn, R. Textural, mineralogical and chemical characteristics of copper reverberatory furnace smelter slag of the Okiep Copper District, South Africa. *Miner. Eng.* **2013**, *52*, 184–190. [[CrossRef](#)]
33. Toffolo, L.; Addis, A.; Martin, S.; Nimis, P.; Rottoli, M.; Godard, G. The Misérègne slag deposit (Valle d’Aosta, Western Alps, Italy): Insights into (pre-)Roman copper metallurgy. *J. Archaeol. Sci. Rep.* **2018**, *19*, 248–260. [[CrossRef](#)]
34. Sulem, J.; Famin, V. Thermal decomposition of carbonates in fault zones: Slip-weakening and temperature-limiting effects. *J. Geophys. Res. Solid Earth* **2009**, *114*, B03309. [[CrossRef](#)]
35. Bourgarit, D.; Mille, B.; Prange, M.; Ambert, P.; Hauptmann, A. Chalcolithic Fahlro Smelting at Cabrières: Reconstruction of Smelting Processes by Archaeometallurgical Finds. In *Proceedings of the Archaeometallurgy in Europe*, Milan, Italy, 24–26 September 2003; Associazione Italiana di Metallurgia: Milan, Italy, 2003; pp. 431–440.
36. Sáez, R.; Nocete, F.; Nieto, J.M.; Capitán, M.Á.; Rovira, S. The extractive metallurgy of copper from Cabezo Juré, Huelva, Spain: Chemical and mineralogical study of slags dated to the third millennium B.C. *Can. Miner.* **2003**, *41*, 627–638. [[CrossRef](#)]
37. Tumiat, S.; Casartelli, P.; Mambretti, A.; Martin, S. The ancient mine of servette Saint-Marcel, Val D’aosta, Western Italian Alps): A mineralogical, metallurgical and charcoal analysis of furnace slags. *Archaeometry* **2005**, *47*, 317–340. [[CrossRef](#)]
38. Álvarez-Valero, A.M.; Pérez-López, R.; Nieto, J.M. Prediction of the environmental impact of modern slags: A petrological and chemical comparative study with Roman age slags. *Am. Miner.* **2009**, *94*, 1417–1427. [[CrossRef](#)]
39. Pelton, A.; Stamatakis, M.G.; Kelepertzis, E.; Panagou, T. The origin and archaeometallurgy of a mixed sulphide ore for copper production on the island of Kea, Aegean Sea, Greece. *Archaeometry* **2015**, *57*, 318–343. [[CrossRef](#)]
40. Warchulski, R. Zn-Pb slag crystallization: Evaluating temperature conditions on the basis of geothermometry. *Eur. J. Miner.* **2016**, *28*, 375–384. [[CrossRef](#)]
41. Cabała, J.; Warchulski, R.; Rozmus, D.; Środek, D.; Szełęg, E. Pb-Rich Slags, Minerals, and Pollution Resulted from a Medieval Ag-Pb Smelting and Mining Operation in the Silesian-Cracovian Region (Southern Poland). *Minerals* **2020**, *10*, 28. [[CrossRef](#)]
42. Humphris, J.; Martín-Torres, M.; Rehren, T.; Reid, A. Variability in single smelting episodes—A pilot study using iron slag from Uganda. *J. Archaeol. Sci.* **2009**, *36*, 359–369. [[CrossRef](#)]
43. Bachmann, H.G. *The Identification of Slags from Archaeological Sites*; Institute of Archaeology Occasional Publication: Ankara, Turkey, 1982.